

ASCAT and QuikSCAT Azimuth Modulation of Backscatter Over East Antarctica

Richard D. Lindsley, *Member, IEEE*, and David G. Long, *Fellow, IEEE*

Abstract—For most land and ice surfaces, the measured radar backscatter at the spatial resolution of a wind scatterometer is insensitive to the azimuth angle. However, for regions of East Antarctica, the backscatter strongly depends on the azimuth angle. This relationship between backscatter and azimuth angle is often modeled with a Fourier series. Although previous work has separately examined the data from QuikSCAT, a Ku-band scatterometer, and the Advanced Scatterometer (ASCAT), a C-band scatterometer, this letter compares the two on the same high-resolution grid. We find that, although QuikSCAT has superior azimuth angle coverage (due to its measurement geometry) compared to ASCAT, both are suitable to estimate the radar backscatter azimuth angle modulation of East Antarctica. The ASCAT data exhibit a much larger azimuth modulation than the QuikSCAT data. This is attributed to the different wavelengths of the microwave signal: At C-band (5.7 cm), East Antarctica has features that show radar backscatter to be more dependent on azimuth angle than at Ku-band (2.2 cm). This letter also examines the ASCAT and QuikSCAT azimuth modulation over previously identified regions of wind glaze. Although azimuth modulation is expected to be minimal over wind glaze, we find the wind-glaze regions to contain more structure than previously suggested.

Index Terms—Advanced Scatterometer (ASCAT), antarctica, ice, QuikSCAT, scatterometer, spaceborne radar.

I. INTRODUCTION

A SCATTEROMETER measures the Earth surface radar backscatter, or σ° , over a distributed area. Each measurement has an associated incidence angle θ and an azimuth angle ϕ . For most land and ice surfaces, σ° depends only on the incidence angle, not on the azimuth angle. However, in regions of East Antarctica associated with megadunes and sastrugi, the physical structures induce a strong azimuth dependence [1]. Conversely, wind-glaze regions in Antarctica are expected to have little azimuth modulation [2]. This azimuth modulation has been previously modeled as a second- or fourth-order Fourier series [3]–[5].

Previous work has explored the azimuth modulation of scatterometer data. Data from the Advanced Scatterometer (ASCAT) are used in [6], where a variety of models are evaluated to fit the incidence and azimuth angle dependence of the σ° data. Physical interpretations for the observed azimuth variation

are explored in [1] and [7] using data from the QuikSCAT and European Remote Sensing (ERS) scatterometers. Modeling the azimuth modulation as a Fourier series, the first-order term typically correlates with the local slope of the surface, whereas the second-order term correlates with sastrugi carved into the ground due to persistent katabatic winds.

Although previous work has described the azimuth modulation of ASCAT data over Antarctica [6], the spatial resolution was limited. Spatially averaged backscatter data (ASCA_SZR_1B product) are used, and the azimuth modulation parameters are retrieved on a polar stereographic projection with a grid spacing of 12.5 km. This letter instead uses the full-resolution data (ASCA_SZF_1B product). A limited form of resolution enhancement is computed through the use of the AVE (weighted AVErage) algorithm on a 3.125-km grid [8]. QuikSCAT data are likewise processed on the same grid in order to compare the azimuth modulation results.

In this letter, we describe the azimuth modulation of ASCAT and QuikSCAT data using a fourth-order Fourier series fit. Enhanced-resolution image reconstruction using the AVE algorithm is applied to estimate the incidence and azimuth dependence of σ° for each pixel. The backscatter model used in this letter and the procedure to estimate the azimuth modulation model parameters are described in Section II. Results are shown in Section III. Section IV concludes this letter.

II. METHOD

ASCAT (2007–present) is a fan-beam C-band (5.255 GHz) scatterometer. Its measurement geometry samples σ° at a wide range of incidence angles ($\approx 30^\circ$ to 60°) but only at limited azimuth angles. QuikSCAT (1999–2009) is a scanning pencil beam scatterometer at Ku-band (13.4 GHz). Because of its different measurement geometry, QuikSCAT observes σ° at only two incidence angles (47° and 54°) but has complete azimuth angle coverage.

While ASCAT only measures σ° at vertical polarization (VV), QuikSCAT measures both vertically and horizontally polarized (VV and HH) σ° . For comparison purposes in this letter, only the VV QuikSCAT data are used. QuikSCAT reports two types of measurements: “egg” data, where the measurement footprint is essentially the antenna response, and “slice” data, which subdivides the antenna pattern using range-Doppler processing [9]. Slice data have a finer spatial resolution but are noisier than egg data.

Over land and sea ice, the dependence of σ° on θ is often described as a linear fit with σ° in log space, such as dB

$$\sigma^\circ(\theta) = \mathcal{A} + \mathcal{B}(\theta - 40^\circ). \quad (1)$$

Manuscript received December 2, 2015; revised April 16, 2016; accepted May 15, 2016. Date of publication June 15, 2016; date of current version July 20, 2016.

R. D. Lindsley was with the Microwave Earth Remote Sensing Laboratory, Brigham Young University, Provo, UT 84602 USA. He is now with Remote Sensing Systems, Santa Rosa, CA 95401 USA (e-mail: lindsley@remss.com).

D. G. Long is with the Department of Electrical and Computer Engineering and the Microwave Earth Remote Sensing Laboratory, Brigham Young University, Provo, UT 84602 USA (e-mail: long@ee.byu.edu).

Color versions of one or more of the figures in this paper are available online at <http://ieeexplore.ieee.org>.

Digital Object Identifier 10.1109/LGRS.2016.2572101

In this model, σ° is decomposed into \mathcal{A} , which is the backscatter normalized to a 40° incidence angle, and \mathcal{B} , which describes the slope of the θ dependence [8], [10]. Since QuikSCAT does not sample over a wide range of incidence angles, QuikSCAT \mathcal{B} is treated as zero, and \mathcal{A} is simply the mean σ° for the pixel.

A previous azimuth modulation study [1] uses a second-order Fourier series to fit the azimuth angle modulation in the residual backscatter after the estimation of \mathcal{A} and \mathcal{B} . Although several azimuth modulation models were considered, in this letter, we use a fourth-order Fourier series with the third-order terms assumed to be zero. The azimuth and incidence angle models together are

$$\sigma^\circ(\theta, \phi) = \sigma^\circ(\theta) + \sigma^\circ(\phi) \quad (2)$$

$$= \mathcal{A} + \mathcal{B}(\theta - 40^\circ)$$

$$+ \sum_{k=\{0,1,2,4\}} B_k \cos(k\phi) + C_k \sin(k\phi). \quad (3)$$

To aid in interpreting the results, the sine and cosine coefficients are converted from rectangular to polar coordinates

$$m_k = \sqrt{B_k^2 + C_k^2} \quad (4)$$

$$\varphi_k = \tan^{-1} \left(\frac{C_k}{B_k} \right). \quad (5)$$

Thus, m_k and φ_k are the k th order azimuth modulation magnitude and phase, respectively. (The term B_0 is an azimuth-modulation bias and is expected to be small; C_0 is defined to be zero.)

A scatterometer measures the Earth surface radar backscatter, or σ° , over a distributed area

$$z_i = \iint \sigma^\circ(x, y) h_i(x, y) dx dy + \eta_i \quad (6)$$

where z_i is the measurement i , $\sigma^\circ(x, y)$ is the Earth surface backscatter, $h_i(x, y)$ is the normalized spatial response function (SRF) for each measurement, and η_i is a per-measurement noise term. Image reconstruction uses the σ° measurements in conjunction with their associated SRFs to reconstruct the true σ° on a high-resolution grid. In this letter, we apply the AVE method, a partial reconstruction approach that uses the weighted average of the SRFs [8].

Using AVE, \mathcal{A} and \mathcal{B} for each pixel j are computed with a simple linear regression. After the estimation of $\mathcal{A}[j]$ and $\mathcal{B}[j]$, the azimuth modulation parameters m_k and φ_k are computed using a linear least squares approach, where each measurement is weighted by the SRF value at the pixel.

III. RESULTS AND DISCUSSION

ASCAT and QuikSCAT data are collected over the Antarctic region for the same date range: days 211–240, 2009 (2009-07-30 to 2009-08-28). This 30-day range is during the Austral winter when no significant melt or refreeze is expected. AVE on a 3.125-km grid spacing is used to estimate the azimuth modulation coefficients.

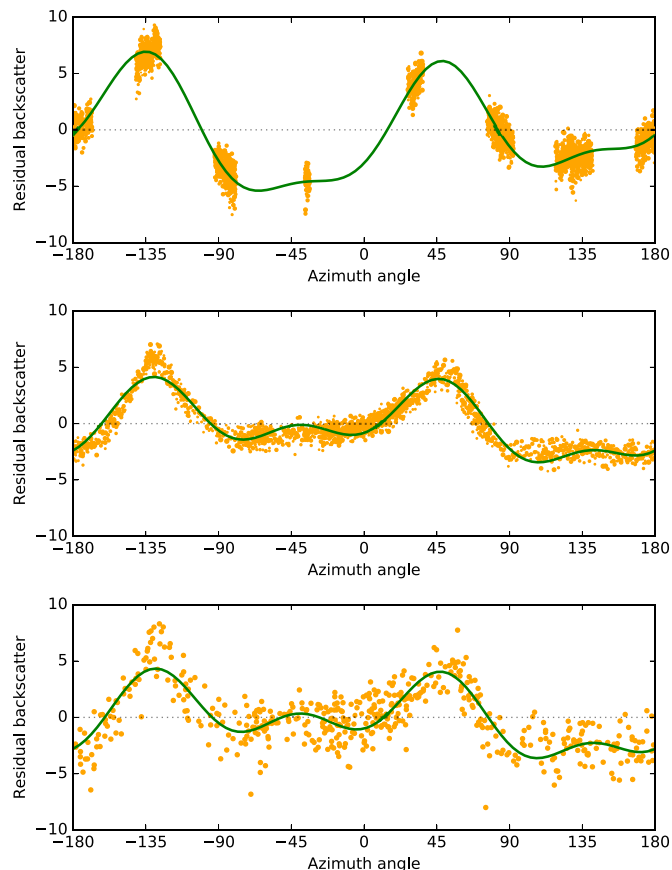


Fig. 1. Residual backscatter values and fourth-order Fourier series fit to the data from a 9.8-km² area at -67.99° N 126.48° E. (Top to bottom) ASCAT, QuikSCAT eggs, and QuikSCAT slices.

TABLE I
ESTIMATED AZIMUTH MODULATION MAGNITUDE AND PHASE COEFFICIENTS FOR THE DATA SHOWN IN FIG. 1. THE m_k TERMS ARE IN DECIBELS, AND THE φ_k TERMS ARE IN DEGREES. THE DATA ARE FROM A 9.8-km² AREA AT -67.99° N 126.48° E.

Coef.	ASCAT	Egg	Slice
m_1	1.42	1.13	1.31
m_2	4.97	2.65	2.58
m_4	1.77	1.49	1.68
φ_1	154	-46	-47
φ_2	87	92	95
φ_4	-165	-164	-161

A. Pixel results

A single high-resolution pixel is first selected, located at -67.99° N 126.48° E. The residual backscatter (i.e., after removing the estimated \mathcal{A} and \mathcal{B} values) at this pixel as a function of azimuth angle is shown in Fig. 1 for ASCAT, QuikSCAT eggs, and QuikSCAT slices. The fourth-order Fourier series fit is also displayed, and the estimated coefficient values are listed in Table I. In Fig. 1, the difference in sampling geometry between ASCAT and QuikSCAT is apparent: For ASCAT, only a few groups of azimuth angles are sampled, but the QuikSCAT azimuth angle coverage is much more dense, with no large gaps present. The QuikSCAT slice values are also much noisier than the QuikSCAT egg values: The residual backscatter values have

more vertical spread. Notwithstanding the noise, the Fourier series fits for the two QuikSCAT cases are similar in this case. (However, this is not true for all pixels in the region.)

Comparing the ASCAT and QuikSCAT values, in all three cases, two large peaks are present at azimuth angles of about -135° and 45° ; however, ASCAT does not have any σ° measurements directly at the center of the 45° peak, only on either side. Conversely, the valley between -90° and 0° is much lower for ASCAT, at about -5 dB, than for QuikSCAT, at about -1 dB. Also, between about 120° and -160° , the QuikSCAT data have a “valley” at about -3 dB, but for ASCAT, it starts to slope upward at 135° . While the two peaks are similar in position and magnitude, the behavior between the peaks is different for QuikSCAT and ASCAT, leading to different estimated values, most significantly larger estimated magnitude terms m_k .

B. Region Results

The azimuth modulation parameters are estimated for the entire Antarctic region, masking out ocean and sea ice. Fig. 2 displays m_1 , m_2 , and m_4 , the modulation magnitudes, and Fig. 3 displays φ_1 , φ_2 , and φ_4 , the modulation phases. Only ASCAT and the QuikSCAT egg data are shown because the QuikSCAT slice data (not shown) are too noisy.

For all images shown in Figs. 2 and 3, the estimated values are less accurate closer to the South Pole at the center of the images. This is due to the polar orbits of QuikSCAT and ASCAT and their measurement geometry. South of about 78° S, the Earth is only measured by one of the two ASCAT swaths, and south of about 89° S, neither swath observes the Earth surface. Between these two latitudes, ASCAT samples σ° at fewer azimuth angles, so the estimated coefficients are less reliable since they suffer from overfitting. A circular discontinuity is visible at 78° S. QuikSCAT does not have such a sharp discontinuity, but it still samples fewer azimuth angles at extreme latitudes, leading to poor estimates of the azimuth modulation parameters.

As illustrated for one pixel in Fig. 1, the second-order magnitude is generally much larger than the first-order and fourth-order magnitudes. This is visible in Fig. 2, noting that different color scales are used for m_2 than for m_1 and m_4 . Also observed in Fig. 1 and tabulated in Table I for a single pixel, the m_1 , m_2 , and m_4 values are smaller for QuikSCAT than for ASCAT. This holds true in Fig. 2 for the entire region, where the modulation magnitudes are larger from ASCAT than from QuikSCAT. In Fig. 3, the estimated phases φ_2 and φ_4 are very similar between QuikSCAT and ASCAT. However, the QuikSCAT-derived φ_1 images are often roughly 180° different from ASCAT. The larger modulation magnitude at C-band versus Ku-band was previously noted in [5] for Greenland, although a comparison was not conducted for Antarctica.

The standard deviation of the residual backscatter before and after azimuth modulation is additionally computed (not shown) to evaluate the impact of modeling azimuth modulation. Over East Antarctica, the mean of the standard deviation decreases from 1.9 to 1.0 dB for ASCAT and from 1.0 to 0.8 dB for QuikSCAT. Including the azimuth modulation effects improves

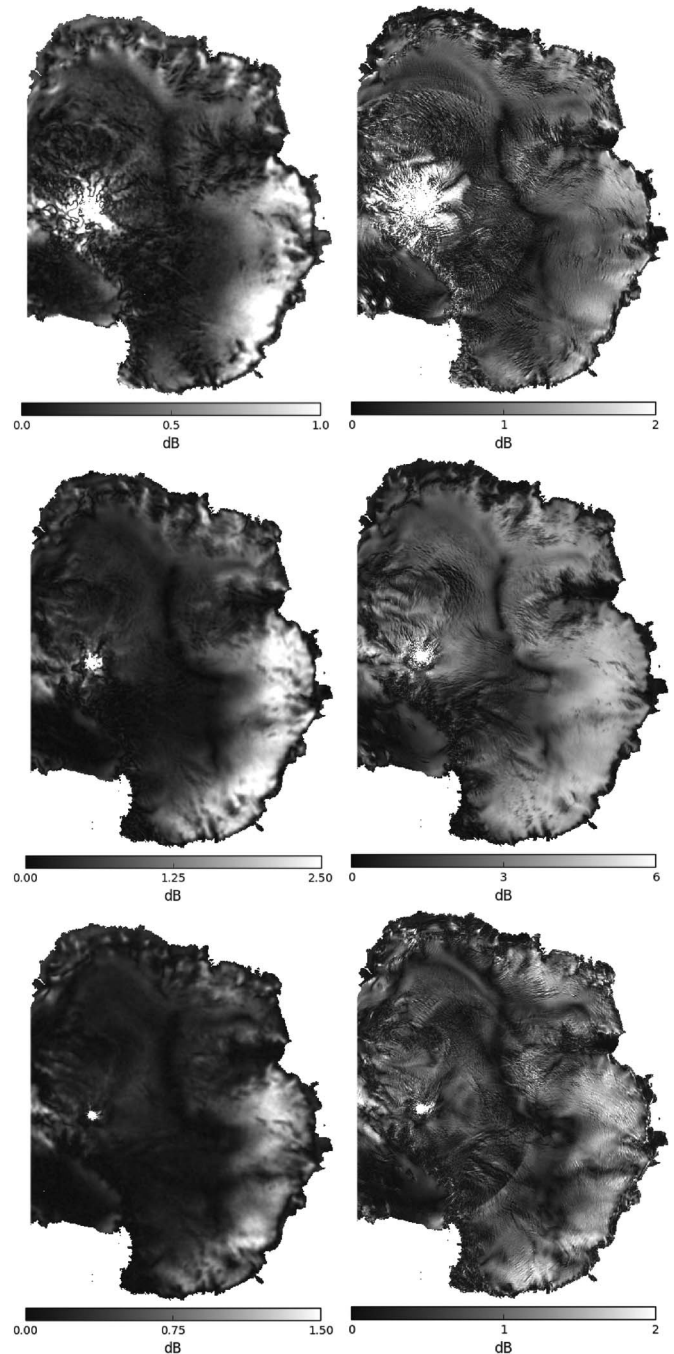


Fig. 2. (Top row) m_1 , (middle row) m_2 , and (bottom row) m_4 azimuth modulation coefficients over Antarctica using 30 days of data. (Left column) QuikSCAT eggs. (Right column) ASCAT. Note that, for clarity, the color scales differ among the images

the model of the scatterometer data, but the effect is more dramatic for ASCAT than for QuikSCAT.

The azimuth modulation parameters estimated from ASCAT and QuikSCAT data share many common features. Areas of higher or lower magnitude, for example, are present in both cases. The consistency of the behavior of magnitudes and phases between ASCAT and QuikSCAT is evidence that the observed azimuth angle modulation is not a scatterometer calibration error or a sampling artifact, but it is due to geophysical

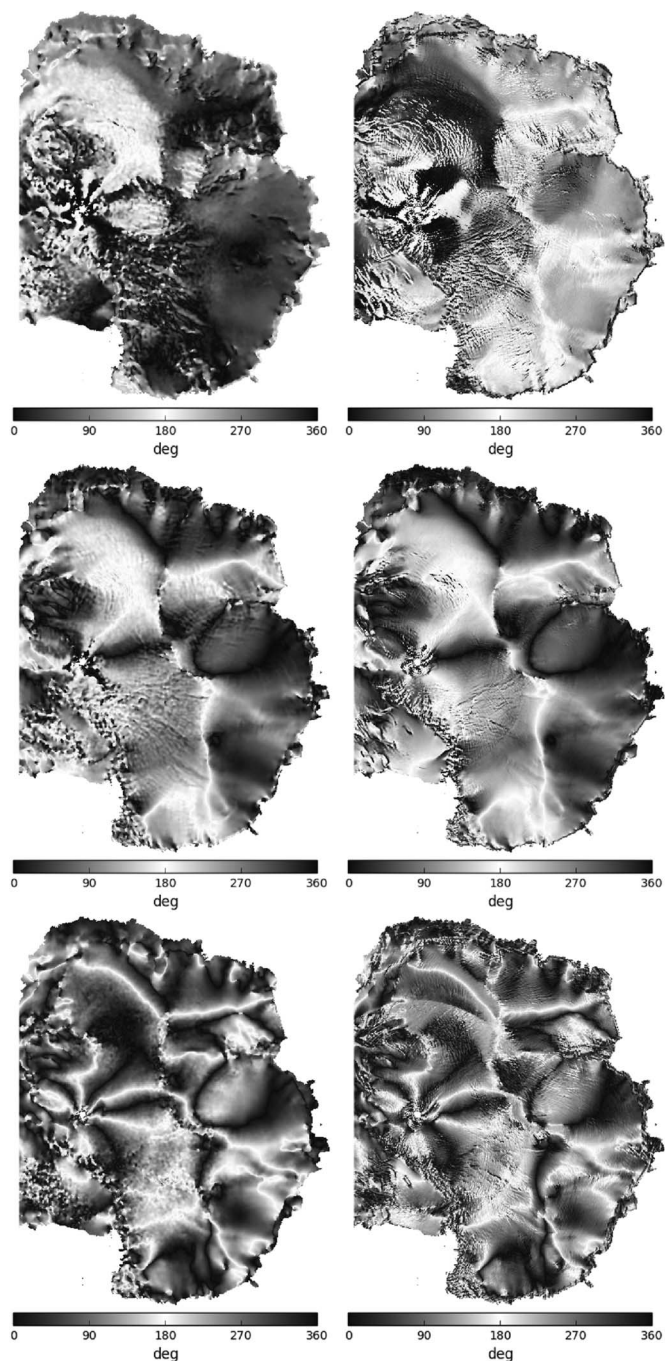


Fig. 3. (Top row) φ_1 , (middle row) φ_2 , and (bottom row) φ_4 azimuth modulation coefficients over Antarctica using 30 days of data. (Left column) QuikSCAT eggs. (Right column) ASCAT.

structures. However, differences exist between the terms estimated by ASCAT and QuikSCAT, even though the two scatterometers observe the same region over the same time range.

The source of the differences is hypothesized to be geophysical. QuikSCAT operates at a wavelength of 2.2 cm, whereas ASCAT is at a 5.7-cm wavelength. The structures in the Antarctic ice sheet that are responsible for azimuth modulation (e.g., sastrugi and megadunes) scatter more strongly at the C-band wavelength of ASCAT than at the Ku-band wavelength of QuikSCAT. Additionally, the penetration depth of snow and

ice is more shallow for QuikSCAT than ASCAT, so ASCAT is subject to more volume scattering than QuikSCAT.

Further study is warranted to understand the reasons behind the differences in azimuth modulation observed by QuikSCAT and ASCAT. However, the enhanced-resolution estimation of the modeled azimuth modulation parameters is an important step. Both QuikSCAT and ASCAT data are consistently produced on the same high-resolution grid using the same Fourier series estimation.

C. Wind-Glaze Regions

A geophysical feature of interest in East Antarctica is the existence of wind-glaze regions. These are areas where the snow surface is polished smooth by blowing snow. Wind-glaze regions are expected to exhibit little to no azimuth modulation [2].

For a region of East Antarctica near the Ross Sea, the ASCAT and QuikSCAT modulation magnitude parameters are shown in Fig. 4, with areas of wind glaze as identified by Scambos *et al.* [2] indicated by the white outlines. Two areas of wind glaze dominate the selected region: one at the upper left corner of the region and one in the right half of the region. The upper left wind-glaze region is identifiable in the ASCAT and QuikSCAT m_k images due to the lower azimuth modulation magnitudes in this region. The other region contains some areas of reduced azimuth modulation but largely exhibits a strong azimuth modulation, similar to the areas without wind glaze.

The results shown in Fig. 4 are representative of other wind-glaze regions: Although some wind-glaze regions exhibit low azimuth modulation magnitude values, other regions have a larger degree of azimuth modulation. Furthermore, the azimuth modulation values are not uniformly dampened within the wind-glaze regions: Large values of azimuth modulation occasionally exist and significant “spotting” and other texture are present at these locations. This suggests a more complicated behavior at these regions, possibly indicating the coexistence of sastrugi or other features so that the mapped wind-glaze regions are not spatially uniform as suggested in [2].

IV. CONCLUSION

The azimuth modulation, or anisotropy, in the observed scatterometer σ° data over East Antarctica is modeled with a Fourier series. Both ASCAT and QuikSCAT data are considered, although QuikSCAT slice data are ultimately not used due to its noise.

The estimated azimuth modulation magnitude and phase terms are similar when comparing ASCAT and QuikSCAT data, although some differences exist. A large difference is that the ASCAT data exhibit a much larger azimuth modulation magnitude than the QuikSCAT data. This is attributed to geophysical structures that are azimuthally anisotropic yet play a larger role at C-band (5.7 cm) for ASCAT than at Ku-band (2.2 cm) for QuikSCAT.

Previously mapped wind-glaze regions are also evaluated for azimuth modulation. We find in both ASCAT and QuikSCAT data that, although less azimuth modulation is typically present within regions of wind glaze, the regions exhibit significant

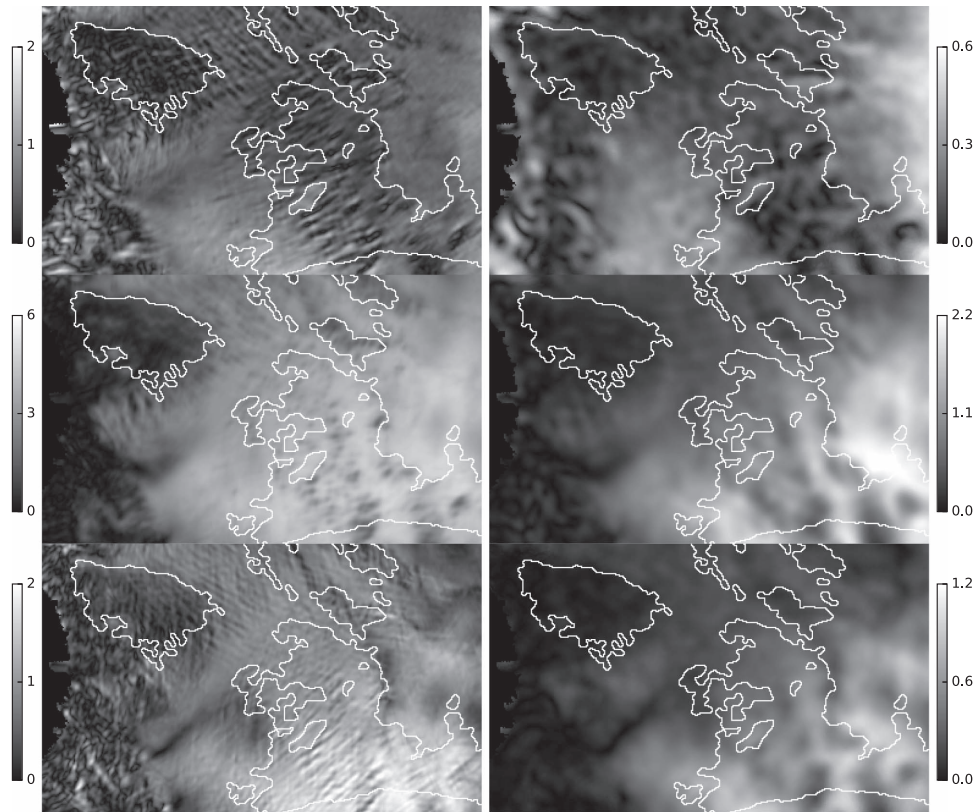


Fig. 4. (Left column) ASCAT and (right column) QuikSCAT egg (top) m_1 , (middle) m_2 , and (bottom) m_4 images over a region of East Antarctica near the Ross Sea. Note that color scales for the images differ to increase image contrast. Wind-glaze regions as mapped by Scambos *et al.* [2] are outlined in white.

variability. Some pixels (each with an area of 9.8 km^2) may contain a modulation magnitude of several decibels.

The results presented here demonstrate the consistency of East Antarctic backscatter azimuth modulation at two radar bands and also illustrate the differences. Furthermore, regions of wind glaze are shown to contain variable azimuth modulation. Future work to better explain the reasons for the differences at C and Ku-bands is needed.

REFERENCES

- [1] D. G. Long and M. R. Drinkwater, "Azimuth variation in microwave scatterometer and radiometer data over Antarctica," *IEEE Trans. Geosci. Remote Sens.*, vol. 38, no. 4, pp. 1857–1870, Jul. 2000.
- [2] T. A. Scambos *et al.*, "Extent of low-accumulation 'wind glaze' areas on the East Antarctic Plateau: Implications for continental ice mass balance," *J. Glaciol.*, vol. 58, no. 210, pp. 633–647, Aug. 2012.
- [3] B. Lambert and D. G. Long, "Seasonal and interannual variations in Antarctic backscatter signature from 2000 to 2006 as observed by QuikSCAT," in *Proc. SPIE Earth Observ. Syst. XII*, Sep. 2007, pp. 1–9.
- [4] I. S. Ashcraft and D. G. Long, "Relating microwave backscatter azimuth modulation to surface properties of the Greenland ice sheet," *J. Glaciol.*, vol. 52, no. 177, pp. 257–266, Mar. 2006.
- [5] D. G. Long, I. S. Ashcraft, and J. B. Luke, "Radar scatterometer observations of sastrugi on the great ice sheets," in *Proc. SPIE Earth Observ. Syst. VIII*, Nov. 2003, pp. 1–9.
- [6] A. D. Fraser, N. W. Young, and N. Adams, "Comparison of microwave backscatter anisotropy parameterizations of the Antarctic ice sheet using ASCAT," *IEEE Trans. Geosci. Remote Sens.*, vol. 52, no. 3, pp. 1583–1595, Mar. 2014.
- [7] Z. Bartalis, K. Scipal, and W. Wagner, "Azimuthal anisotropy of scatterometer measurements over land," *IEEE Trans. Geosci. Remote Sens.*, vol. 44, no. 8, pp. 2083–2092, Aug. 2006.
- [8] R. D. Lindsley and D. G. Long, "Enhanced-resolution reconstruction of ASCAT backscatter measurements," *IEEE Trans. Geosci. Remote Sens.*, vol. 54, no. 5, pp. 2589–2601, May 2016.
- [9] M. W. Spencer, C. Wu, and D. G. Long, "Improved resolution backscatter measurements with the SeaWinds pencil-beam scatterometer," *IEEE Trans. Geosci. Remote Sens.*, vol. 38, no. 1, pp. 89–104, Jan. 2000.
- [10] D. G. Long, P. Hardin, and P. Whiting, "Resolution enhancement of spaceborne scatterometer data," *IEEE Trans. Geosci. Remote Sens.*, vol. 31, no. 3, pp. 700–715, May 1993.